Nonintegrability for $\mathcal{N}=1$ SCFTs in 5D

Dibakar Roychowdhury*

Department of Physics, Indian Institute of Technology Roorkee, Roorkee 247667, Uttarakhand, India

(Received 11 July 2021; accepted 8 September 2021; published 4 October 2021)

We explore the Liouvillian nonintegrability criteria for long quiver gauge theories which preserve $\mathcal{N}=1$ supersymmetry in $5D$. We probe type IIB solutions with (an AdS_6 factor) semiclassical strings which capture the strong coupling dynamics of $\mathcal{N}=1$ superconformal field theories (SCFTs) in $5D$. Our analysis reveals an underlying nonintegrable structure within some sub-sector of these $5D$ SCFTs. To solidify our claim, we complement our analytic results through numerics. We estimate various chaos indicators for the phase space which confirm the onset of a chaotic motion for these type IIB strings.

DOI: 10.1103/PhysRevD.104.086010

I. OVERVIEW AND MOTIVATION

A. Type IIB solutions with AdS_6 factor

Among the plethora of examples of superconformal field theories (SCFTs) that exist in diverse dimensions [and preserve different amounts of supersymmetry (SUSY)], $\mathcal{N}=1$ SCFTs in five dimesions are of particular interest. Starting with the seminal work due to Seiberg [1] and thereby subsequently followed by authors in [2–4], recently this particular class of SCFTs has attracted a lot of attention in the context of the holographic correspondence.

The bulk dual of these SCFTs is realized as a type IIB solution with an AdS_6 factor those preserving only half of the total 32 supersymmetries in $10D$. In the original construction of [5–7], these type IIB solutions were realized as a warped product of the form $\mathrm{AdS}_6\times S^2\times\Sigma_{(2)}$ where $\Sigma_{(2)}$ is a two-dimensional Riemann surface parametrized by means of some complex coordinates $(z,\bar{z})$. Furthermore, in the original constructions of [5–7], the warped factors of AdS_6 as well as S^2 line elements are defined in terms of the locally holomorphic functions on the two-dimensional Riemann surface $(\Sigma_{(2)})$.

Following these developments, several other aspects of $\mathcal{N}=1$ quiver gauge theories in $5D$ have been explored in the recent years. Let us review some of these results here.

A large class of $5D$ SCFTs and the RG flow between these theories have been explored recently by authors in [8]. Their analysis reveals an intriguing fact; namely they show that the sphere-free energy for these theories decreases as one RG flows from UV to IR.

Codimension 2 (surface) defects in $5D$ SCFTs have been investigated by authors in [9] using (p,q) five brane webs with D3-branes. In a related study, nonlocal operators, for example Wilson loops in $5D$ SCFTs have been constructed in [10]. Other than these, a series of papers [11–15] have been put forward in the recent years those explore various other properties of these $5D$ SCFTs using type IIB solutions in $10D$.

In spite of these developments, several other field theoretic aspects of $5D$ SCFTs are yet to be addressed. One of these aspects include the possibility of finding integrability for these $5D$ fixed points. In a holographic set up, this translates into an equivalent question of showing integrability for the classical $2D$ world sheet theory on $\mathrm{AdS}_6\times S^2\times\Sigma_{(2)}$.

Showing classical integrability for $2D$ sigma models is in general is a difficult task as there is no general prescription for writing down the corresponding Lax pairs. An alternative approach might therefore be disproving the classical integrability for these type IIB strings on $\mathrm{AdS}_6\times S^2\times\Sigma_{(2)}$. For the purpose of the present paper, we choose to work with this second path where we probe the internal manifold of the full type IIB background by various wrapped string configurations. In a holographic framework, these solitons capture the dynamics of long/heavy single trace operators in the dual $5D$ SCFTs. The idea is to check the classical nonintegrability for each of these configurations.

In this work, we adopt the recently proposed electrostatic viewpoint [16] of type IIB solutions with an AdS_6 factor.[1] Following this, we first review the basics of this

*dibakarphys@gmail.com, dibakar.roychowdhury@ph.iitr.ac.in

[1]Typically, in an "electrostatic description" one classifies the quiver using the so called *Rank* function $[\mathcal{R}(\eta)]$ which encodes all the information about the color and flavor nodes of the quiver. In electrostatic approach of [16], one can embed the $\mathcal{N}=1$ quivers in a Hanany-Witten brane setup that comprises of NS5-D5-D7–brane intersections in $10D$. Here D5s correspond to the color nodes of the quiver whereas on the other hand, D7s are the flavor branes localized along the internal manifold of the type IIB background. For example, in this language $\tilde{T}_{N_c,P}$ quivers are characterized by a linearly increasing Rank function $[\mathcal{R}(\eta)=N_c\eta]$ for $0\leq\eta\leq(P-1)$ which is closed at $\eta=P$ by placing flavor branes at $\eta=P-1$.

electrostatic framework of type IIB solutions which preserve $\mathcal{N}=1$ SUSY. The full $10D$ solution may be expressed in terms of an AdS_6 factor together with some internal manifold ($\mathcal{M}_4$) that [contains a two sphere (S^2)] preserves the $SU(2)_R$ symmetry of the dual SCFTs in $5d$. In our analysis, we probe this internal space with various semiclassical $F1$ strings.

The type IIB background, that we choose to work with can be related to those obtained in [17] through S duality [16]. In the string frame, the type IIB background reads as[2] [16]

$$ds^2_{IIB} = f_1(\sigma,\eta) ds^2_{\mathrm{AdS}_6} + ds^2_{\mathcal{M}_4} \tag{1}$$

$$= f_1(\sigma,\eta) ds^2_{\mathrm{AdS}_6} + f_2(\eta,\sigma) d\Omega_2(\chi,\xi) + f_3(\eta,\sigma)(d\sigma^2 + d\eta^2) \tag{2}$$

$$B_2 = f_4(\sigma,\eta)\sin\chi d\chi \wedge d\xi; \quad \mathcal{C}_2 = f_5(\sigma,\eta)\sin\chi d\chi \wedge d\xi \tag{3}$$

$$e^{-2\phi} = f_6(\sigma,\eta); \quad \mathcal{C}_0 = f_7(\sigma,\eta) \tag{4}$$

$$f_1 = \frac{3\pi}{2}\left(\sigma^2 + \frac{3\dot{V}}{\partial^2_\eta V}\right)^{1/2}; \quad f_2 = f_1 \frac{\partial^2_\eta V \dot{V}}{3\sigma\Delta}; \quad f_3 = f_1 \frac{\partial^2_\eta V}{3\dot{V}} \tag{5}$$

$$f_4 = \frac{\pi}{2}\left(\eta - \frac{\dot{V}\partial_\sigma\partial_\eta V}{\Delta}\right); \quad f_5 = \frac{\pi}{2}\left(V - \frac{\dot{V}}{\Delta}(\partial_\eta V(\partial_\sigma\partial_\eta V) - 3\partial^2_\eta V \partial_\sigma V)\right) \tag{6}$$

$$f_6 = \frac{12\sigma\dot{V}\partial^2_\eta V\Delta}{(3\partial_\sigma V + \sigma\partial^2_\eta V)^2}; \quad f_7 = 2\left(\partial_\eta V + \frac{3\dot{V}\partial_\sigma\partial_\eta V}{(3\partial_\sigma V + \sigma\partial^2_\eta V)}\right) \tag{7}$$

$$\Delta = \frac{1}{\sigma}(2\dot{V} - \ddot{V})\partial^2_\eta V + \sigma(\partial_\sigma\partial_\eta V)^2; \quad \dot{V}(\sigma,\eta) = \sigma\partial_\sigma V. \tag{8}$$

The Bogomol'nyi-Prasad-Sommerfield conditions yield the following partial differential equation for the potential function $V(\sigma,\eta)$

$$\partial_\sigma(\sigma^2\partial_\sigma V) + \sigma^2\partial^2_\eta V = 0, \tag{9}$$

that is required to be solved with appropriate boundary conditions namely

$$\hat{V}(\sigma \to \pm\infty, \eta) = 0; \quad \mathcal{R}(\eta = 0) = 0 = \mathcal{R}(\eta = P). \tag{10}$$

The potential function $\hat{V} = \sigma V$ satisfies Laplace equation of electrostatics with the boundary conditions

$$\hat{V}(\sigma, \eta = 0) = 0 = \hat{V}(\sigma, \eta = P) \tag{11}$$

where the range for holographic direction (η) is bounded between 0 and P. Given the above electrostatic equivalence, one can interpret $\mathcal{R}(\eta)$ as the charge distribution [along the holographic axis (η)] between two conducting planes placed at $\eta = 0$ and $\eta = P$ [16].

The Hanany-Witten set up corresponding to (1)–(8) consists of an intersection of NS5-D5-D7–brane configuration in $10d$. Clearly, the corresponding $\mathcal{N}=1$ superconformal quiver must end at $\eta = P$ which is achieved by placing flavor D7-branes at that point.

In the present paper, we restrict ourselves to $\sigma \sim 0$ plane while moving along the η direction of $\mathcal{M}_4$. Namely, we consider a legitimate expansion of the potential function $\hat{V}(\sigma,\eta)$ near $\sigma \sim 0$ and estimate the corresponding metric functions $f_i(\sigma,\eta)$. Under such circumstances, one therefore expects a charge distribution between the conducting planes at $\eta = 0$ and $\eta = P$. This depends on the location of the flavor D7-branes along the η axis of $\mathcal{M}_4$. This is equivalent of saying that the corresponding rank function ($\mathcal{R}(\eta)$) of the associated $SU(N_c)$ color (gauge) group is piecewise linear in the interval $0 \le \eta \le P$.

B. Summary of results

Given the above set up (1)–(8), below we summarize the key findings of the paper. We explore the strong coupling dynamics of $\mathcal{N}=1$ linear quivers by probing the type IIB geometry (1)–(8) with various semiclassical $F1$ string configurations.

(a) Our analysis reveals an intriguing fact—while certain long operators (at strong coupling) exhibit a simple set of dispersion relations, the $\mathcal{N}=1$ superconformal fixed point (in $5D$) in general maintains some underlying nonintegrable structure with it. We confirm this nonintegrable structure using both analytic as well as numeric techniques.

(b) The analytic technique that we implement in this paper is based on the rigorous mathematical formalism due to Kovacic[3] [18–19] that has been applied (in order to unfold nonintegrability for a wider class of supersymmetric gauge theories in diverse dimensions) with a remarkable success in the recent years [20–27].

Following the methodology as discussed in [20–21], we propose a consistent $1D$ reduction of type IIB sigma model that fails to be compatible with the criteria set by Kovacic which therefore disproves

[2]See Appendix B of [16] for an illuminating discussion on the mapping of type IIB solutions (1)–(8) to the original construction by authors in [5]. This shows the equivalence between these two approaches.

[3]See Section III A for a brief discussion on the algorithm due to Kovacic.

the Liouvillian integrability of the sigma model in general. By virtue of the holographic correspondence, this translates into the simple fact of the nonexistence of the integrable structure for some specific (sub) sector of $\mathcal{N} = 1$ SCFTs in $5D$.

(c) In order to solidify our claim, we complement our analytic results through numerical studies where we estimate various chaos indicators [28–29] for the theory under consideration. Our analysis reveals that the nonintegrability in $\mathcal{N} = 1$ SCFTs triggers a chaotic motion associated with the phase space trajectories of the type IIB (super)strings which in turn also destroys the so called Kolmogorov-Arnold-Moser (KAM) tori [30–31] of integrable string trajectories.

(d) We now summarize our results by referring to the different sections of the paper. In Sec. II we explore certain class of long operators in $\mathcal{N} = 1$ SCFTs which are dual to folded fundamental ($F1$) strings which are allowed to pass through localized flavor D7-branes along the internal space of the full type IIB solution. Our analysis reveals a set of simple dispersion relations for these long operator states.[4]

However, the main analysis of our paper refers to Sec. III where we focus on a particular winding string ansatz that wraps the isometry of the internal two sphere ($S^2 \subset \mathcal{M}_4$) and fluctuates along the rest of the directions of the internal manifold ($\mathcal{M}_4$). We show that a consistent $1D$ reduction of the original sigma model fails to be compatible with the analytic integrability criteria set by the Kovacic's algorithm [18–19].

In Sec. IV we further explore on the nature of this nonintegrable deformation at the level of the Hamiltonian dynamics. We estimate various chaos indicators for example, the Lyapunov exponent as well as the Poincaré section which together confirm the onset of a chaotic dynamics for these type IIB strings.

Finally, we put forward some future remarks and draw our conclusion in Sec. V.

II. SPECTRUM OF LONG OPERATORS IN $\mathcal{N} = 1$ SCFTs

We begin with the description of extended (as well as folded) $F1$ string configurations that probe type IIB geometry (1) along the η axis. While extended along the η direction, these strings naturally meet the stack of flavor D7-branes which are localized along $\mathcal{M}_4$. Our goal would be to explore the imprint of these flavor D7-branes on the associated spectrum of long operators pertaining to $\mathcal{N} = 1$ superconformal quivers at strong coupling.

In the supergravity approximation, these long (single-trace) operators are dual to folded $F1$ strings whose dynamics is encoded in the following sigma model action[5]

$$S_P = \frac{1}{4\pi}\int d\tau d\tilde{\sigma}\mathcal{L}_P, \tag{12}$$

$$\mathcal{L}_P = -G_{MN}\partial_\tau X^M \partial_\tau X^N + G_{MN}\partial_{\tilde{\sigma}} X^M \partial_{\tilde{\sigma}} X^N + 2B_{MN}\partial_\tau X^M \partial_{\tilde{\sigma}} X^N, \tag{13}$$

where we restrict ourselves only to the metric as well as the NS-NS sector of the full type IIB solution (1)–(8).

The above Lagrangian (13) is supplemented with the Virasoro constraints of the following form

$$T_{\tau\tau} = T_{\tilde{\sigma}\tilde{\sigma}} = G_{MN}\partial_\tau X^M \partial_\tau X^N + G_{MN}\partial_{\tilde{\sigma}} X^M \partial_{\tilde{\sigma}} X^N = 0, \tag{14}$$

$$T_{\tau\tilde{\sigma}} = G_{MN}\partial_\tau X^M \partial_{\tilde{\sigma}} X^N = 0. \tag{15}$$

A. Long strings

To start with, we place F1 strings near the center ($\rho \sim 0$) of global AdS_6. In particular, we consider long folded string configurations those are extended through the flavor D7-branes while simultaneously wrapping the S^2 along its equatorial plane.

These strings are therefore described by an embedding of the following form,

$$t = \tau; \quad \eta = \eta(\tilde{\sigma}); \quad \sigma = \sigma(\tilde{\sigma}); \quad \chi = \frac{\pi}{2}; \quad \xi = \ell\tilde{\sigma}. \tag{16}$$

Given the above configuration (16), these strings are naturally decoupled from the background NS-NS fluxes. The effects of incorporating NS-NS coupling will be discussed in the subsequent sections.

Below we summarize the set of equations that readily follows from (13)

$$2f_3\sigma'' = \partial_\sigma f_3(\eta'^2 - \sigma'^2) - 2\partial_\eta f_3\eta'\sigma' + \partial_\sigma f_1 + \ell^2\partial_\sigma f_2, \tag{17}$$

$$2f_3\eta'' = \partial_\eta f_3(\sigma'^2 - \eta'^2) - 2\partial_\sigma f_3\eta'\sigma' + \partial_\eta f_1 + \ell^2\partial_\eta f_2, \tag{18}$$

where the prime corresponds to derivative with respect to $\tilde{\sigma}$.

The above set of equations (17)–(18) are supplemented with Virasoro constraints of the following form

$$T_{\tau\tau} = T_{\tilde{\sigma}\tilde{\sigma}} = -f_1 + \ell^2 f_2 + f_3(\eta'^2 + \sigma'^2) = 0, \tag{19}$$

$$T_{\tau\tilde{\sigma}} = 0. \tag{20}$$

[4] See Appendix A for a detailed discussion on the Liouvillian (non)integrable structure for this particular stringy configuration.

[5] We set $\alpha' = g_s = 1$.

Below we explore the above set of equations (17)–(19) for different choices of the $\mathcal{N}=1$ linear quivers those were proposed recently in [16].

1. $\tilde{T}_{N_c,P}$ quivers

The first example we consider is that of single-kink quivers ($\tilde{T}_{N_c,P}$) which are closed at $\eta = P$ by placing flavor D7-branes at $\eta = P-1$.

The corresponding rank function is given by

$$\mathcal{R}(\eta) = \begin{cases} N_c\eta & 0 \le \eta \le (P-1) \\ N_c(P-1)(P-\eta) & (P-1) \le \eta \le P. \end{cases} \tag{21}$$

In the supergravity approximation the associated potential function reads as [16]

$$\hat{V}(\sigma\sim 0,\eta) \sim \frac{\eta N_c P\log 2}{\pi} - \frac{\pi\eta(\eta^2+1)N_c}{24P} - \frac{\sigma\eta N_c}{2} + \mathcal{O}(\sigma^2/P), \tag{22}$$

where the above expansion (22) is valid in the regime where σ is finite and $P \gg 1$.

On the other hand, an expansion near $|\sigma| \to \infty$ reveals a potential function of the following form[6]

$$\hat{V}(\sigma\to\infty,\eta) \sim \frac{P^3 N_c}{\pi^3} e^{-\frac{\pi\sigma}{P}} \sin\left(\frac{\pi}{P}\right)\sin\left(\frac{\pi\eta}{P}\right). \tag{23}$$

Below, we explore the regime $\sigma \sim 0$. The corresponding metric functions $[f_i(\sigma,\eta)]$ read as

$$f_1(\sigma\sim 0,\eta) \sim \frac{3\pi}{2}\sqrt{-\frac{\eta^2}{2} + \frac{12P^2\log 2}{\pi^2} - \frac{1}{2}} + \mathcal{O}(\sigma^2), \tag{24}$$

$$f_2(\sigma\sim 0,\eta) \sim \frac{-3(\pi^2\eta^2(24P^2\log 2 - \pi^2(\eta^2+1))^{3/2})}{\sqrt{2}(\pi^4(9\eta^4+12\eta^2-1) - 576P^4\log^2 2 + 48\pi^2(1-6\eta^2)P^2\log 2)}, \tag{25}$$

$$f_3(\sigma\sim 0,\eta) \sim \frac{3\pi^2}{\sqrt{48P^2\log 2 - 2\pi^2(\eta^2+1)}} + \mathcal{O}(\sigma^2), \tag{26}$$

which clearly reveals that $\partial_\sigma f_i(\sigma\sim 0,\eta)\sim 0$. Therefore, $\sigma = \sigma' = \sigma'' = 0$ is a natural solution of (17).

Using the above as the primary input, we compute the energy (E_{sk}) associated with the folded string configuration which is dual to the conformal dimension associated with long operators in $\mathcal{N}=1$ single-kink quivers at strong coupling

$$\hat{\Delta}_{sk} \sim E_{sk} \sim \frac{1}{\pi}\int_0^P f_1 \frac{d\eta}{\eta'} \sim \int_0^P d\eta \frac{f_1}{\sqrt{\Lambda_{sk}}}, \tag{27}$$

where, we set the winding number $\ell = 1$ together with

$$\Lambda_{sk}(\eta,P) \sim P^2\log(4096) - \frac{1}{2}\pi^2(3\eta^2+1) + \frac{7\pi^4\eta^4}{P^2\log(4096)} + \cdots, \tag{28}$$

$$f_1(\eta,P) \sim 3P\sqrt{\log 8} - \frac{\pi^2(\eta^2+1)\sqrt{\frac{3}{\log 2}}}{16P} + \cdots. \tag{29}$$

In view of (28)–(29), we see that the integral (27) yields a finite answer

$$\hat{\Delta}_{sk}|_{P\gg 1} \sim \frac{3P}{2} \sim \frac{3}{2N_c} Q_{D7} \tag{30}$$

which shows that the dimension of the dual operator grows linearly with the size of the quiver. Here, $Q_{D7} = PN_c$ is the Page charge associated with flavor D7-branes [16].

A simple interpretation of the above result (30) comes from a closer inspection of the sigma model potential for $F1$ strings near flavor D7-branes. This readily follows from the Lagrangian density (13)

$$V_{\rm eff}(\eta,P) \sim 3P\sqrt{\log 8} + \frac{\pi^2(3\eta^2-1)\sqrt{\frac{3}{\log 2}}}{16P} + \cdots, \tag{31}$$

which shows that the potential is regular across the location of D7-branes. In other words, the $F1$ string can smoothly pass through flavor D7-branes without exhibiting any divergences in the spectrum.

2. $+_{P,N_c}$ quivers

The second example we consider is that of a linear quiver ($+_{P,N_c}$) with a plateau region which corresponds to placing stack of flavor D7-branes at $\eta = 1$ and $\eta = P-1$. As we shall see shortly that these quivers seek special attention around the position $\eta \sim 1$.

[6]See Appendix B for a detailed discussion on the large σ limit.

The corresponding rank function reads as

$$\mathcal{R}(\eta)=\begin{cases} N_c\eta & 0\le\eta\le 1\\ N_c & 1\le\eta\le(P-1)\\ N_c(P-\eta) & (P-1)\le\eta\le P. \end{cases} \tag{32}$$

The associated potential function when expanded near $\sigma\sim 0$ reads as

$$\frac{\hat{V}(\sigma,\eta)}{(\frac{N_c}{4\pi})}\sim\eta(6+4\log 2)-4\eta\log\left(\frac{\pi}{P}\right)-2\eta\log|1-\eta^2| -(1+\eta^2-\sigma^2)\log\left|\frac{\eta+1}{\eta-1}\right|, \tag{33}$$

where we have taken into account the large $P(\gg 1)$ limit.

A careful analysis reveals that the potential function (33)

$$\frac{\hat{V}(\sigma\sim 0,\eta\sim 1)}{(\frac{N_c}{4\pi})}\sim 6-4\log\left(\frac{\pi}{P}\right)+\mathcal{O}(\eta-1) \tag{34}$$

is indeed regular across the location of flavor D7-branes at $\eta=1$. As a result, one should expect that the corresponding metric functions $[f_i(\sigma,\eta)]$ to be regular across $\eta\sim 1$.

In order to estimate the η integral as before, we therefore divide the entire domain of definition into three regions namely (I) Region I ($0\le\eta\le 1-\delta$), (II) Region II ($1-\delta\le\eta\le 1+\delta$), and (III) Region III ($1+\delta\le\eta\le P$) where the parameter δ is set to be zero towards the end of the calculation.

After a careful analysis, the metric functions corresponding Region I turn out to be

$$f_1(\sigma\sim 0,\eta<1)\sim\frac{3}{2}\pi\sqrt{-\frac{\eta^2}{2}-3\log\left(\frac{\pi}{P}\right)+3+\log 8}, \tag{35}$$

$$f_2(\sigma\sim 0,\eta<1)\sim-\frac{\pi\eta^2(-\eta^2-6\log(\frac{\pi}{P})+6+\log(64))^{3/2}}{3(\sqrt{2}(\eta^4+8\eta^2(\log(\frac{\pi}{2P})-1)-4(\log(\frac{\pi}{2P})-1)^2))}, \tag{36}$$

$$f_3(\sigma\sim 0,\eta<1)\sim-\frac{3\left(\pi\sqrt{-\frac{\eta^2}{2}-3\log(\frac{\pi}{P})+3+\log(8)}\right)}{\eta^2+6\log(\frac{\pi}{P})-3(2+\log(4))}. \tag{37}$$

Let us now explore spacetime solutions in Region II which reveals

$$f_1(\sigma\sim 0,\eta\sim 1)\sim\frac{3\sqrt{3}\pi}{\sqrt{2}}k_c\sqrt{\left|2\log\left(\frac{\pi}{P}\right)-3\right|}, \tag{38}$$

$$f_2(\sigma\sim 0,\eta\sim 1)\sim\frac{1}{9}f_1(\sigma\sim 0,\eta\sim 1), \tag{39}$$

$$f_3(\sigma\sim 0,\eta\sim 1)\sim\frac{9\pi^2}{4}f_1^{-1}(\sigma\sim 0,\eta\sim 1), \tag{40}$$

where the ratio, $\frac{\delta}{\sigma}=k_c$ is kept fixed in the limit $\delta\to 0$, $\sigma\to 0$.

Finally, we note down metric functions corresponding to Region III. These solutions are a bit lengthy and are therefore summarized in the Appendix C.

Combining all these pieces together, the conformal dimension of the dual operator can be computed by performing the η integral piece wise

$$\hat{\Delta}_{qp}\sim\frac{1}{\pi}\int_0^{1-\delta}f_1\frac{d\eta}{\eta'}+\frac{1}{\pi}\int_{1-\delta}^{1+\delta}f_1\frac{d\eta}{\eta'}+\frac{1}{\pi}\int_{1+\delta}^{P}f_1\frac{d\eta}{\eta'}. \tag{41}$$

The first two terms on the right-hand side of (41) are comparatively easy to evaluate. Notice that in each of these integrals η' can be substituted using the constraint (19). Computing the first two integrals in the holographic limit ($\frac{\pi}{P}\ll 1$) we find,

$$\hat{\Delta}_{qp}\sim\frac{\zeta(P)}{2N_c}Q_{D7};\quad Q_{D7}=2N_c \tag{42}$$

$$\zeta(P)=\frac{3}{2}+\frac{1}{\pi}\int_1^P f_1\frac{d\eta}{\eta'}, \tag{43}$$

while the remaining integral is indeed difficult to evaluate for the entire range $1\le\eta\le P$. However, it is noteworthy to mention that in the holographic limit ($P\gg 1$) the dominant contribution to $\zeta(P)$ comes from this remaining integral.

One can perform numerical integration which reveals the following set of data

$$\frac{1}{\pi}\int_1^P f_1 \frac{d\eta}{\eta'} = \begin{cases} 156.603 & P = 100 \\ 235.671 & P = 150 \\ 314.739 & P = 200. \end{cases} \tag{44}$$

From the above set of data, it is clear that for an increase $\Delta P = 50$ there is an uniform increase ($\sim$79) in the corresponding value of the integral (44). In other words, the function $\zeta(P)$ increases linearly with P with a slope $\sim\frac{3}{2}$. Therefore the energy of the quiver is roughly proportional to the size of the quiver

$$\hat{\Delta}_{qp}|_{P\gg1} \sim \frac{3}{2}P. \tag{45}$$

This is precisely what we have seen in the case of single-kink quivers (30).

B. Adding R charge

We now generalize the previous analysis in the presence of nonzero R-charge (J) which is the Cartan of the $SU(2)_R$ symmetry of the internal S^2. In the dual stringy picture this corresponds to rotation of the string along the isometry direction of S^2.

The ansatz that we propose is of the form,

$$t = \tau; \quad \eta = \eta(\tilde{\sigma}); \quad \chi = \frac{\pi}{2}; \quad \xi = \omega\tau, \tag{46}$$

where, to begin with we set $\sigma = \sigma' = \sigma'' = 0$ as this turns out to be a solution of the resulting equations of motion. This is the simplest configuration that one could imagine where the string is stretched along the holographic (η) axis while also rotating along ξ.

The corresponding Lagrangian density is given by[7]

$$\mathcal{L}_P = f_1 - \omega^2 f_2 + f_3\eta'^2 \tag{47}$$

which is supplemented with the Virasoro constraints of the following form

$$T_{\tau\tau} = T_{\tilde{\sigma}\tilde{\sigma}} = -f_1 + \omega^2 f_2 + f_3\eta'^2 = 0, \tag{48}$$

$$T_{\tau\tilde{\sigma}} = 0. \tag{49}$$

Given the above set up, below we estimate the energy (Δ) as well as the R-charge (J) associated with long operators corresponding to each of the above quivers.

[7]In the subsequent analysis we set $\omega = 1$ without any loss of generality.

1. $\tilde{T}_{N_c,P}$ quivers

Given the single-kink quivers as depicted in (21), the energy ($\hat{\Delta}_{sk}$) associated with the dual operator remains the same as in (30).

On the other hand, the R-charge corresponding to these dual operators is given by,

$$J = -\frac{1}{4\pi}\int_0^{2\pi} d\tilde{\sigma}\frac{\delta\mathcal{L}_P}{\delta\dot{\xi}} = \frac{1}{\pi}\int_0^P f_2\frac{d\eta}{\eta'} = \int_0^P d\eta\frac{f_2}{\sqrt{\Lambda_{sk}}}, \tag{50}$$

where, in the holographic limit the denominator is given by an expansion of the form (28).

The numerator (24), on the other hand, can be expanded as

$$f_2(\sigma\sim 0,\eta)|_{P\gg1} \sim \frac{\pi^2\eta^2\sqrt{\frac{3}{\log 2}}}{4P} + \mathcal{O}(1/P^3). \tag{51}$$

Substituting (51) into (50) we finally obtain

$$J \sim \frac{\pi^2 P}{24\log 2}. \tag{52}$$

Combining (30) with (52), we therefore conclude

$$\hat{\Delta}_{sk} \sim \frac{36\log 2}{\pi^2}J \sim 2J. \tag{53}$$

2. $+_{P,N_c}$ quivers

A similar calculation as before reveals,

$$J \sim \frac{1}{\pi}\int_0^{1-\delta} f_2\frac{d\eta}{\eta'} + \frac{1}{9\pi}\int_{1-\delta}^{1+\delta} f_1\frac{d\eta}{\eta'} + \frac{1}{\pi}\int_{1+\delta}^{P} f_2\frac{d\eta}{\eta'}. \tag{54}$$

Like before, the dominant contribution to (54) comes from the integral in the range $1\le\eta\le P$. We evaluate this integral numerically for three different choices of P

$$\frac{1}{\pi}\int_1^P f_2\frac{d\eta}{\eta'} = \begin{cases} 15.7793 & P = 100 \\ 23.7034 & P = 150 \\ 31.6258 & P = 200, \end{cases} \tag{55}$$

which reveals that with an increase $\Delta P = 50$, the value of J increases by an amount $\sim$8.

Therefore, we propose that in the large $P(\gg 1)$ limit

$$J \sim \frac{4}{25}P. \tag{56}$$

Combining (56) with (45) we find

$$\hat{\Delta}_{qp} \sim \frac{75}{8}J \sim 9J. \tag{57}$$

C. Adding NS-NS flux

We now generalize our previous analysis by coupling the sigma model with background NS-NS fluxes. Like before, we restrict ourselves to the $\sigma=0$ plane and propose an embedding of the following form

$$t=\tau;\quad \eta=\eta(\tilde{\sigma});\quad \chi=\chi(\tilde{\sigma});\quad \xi=\tau, \tag{58}$$

which corresponds to extended $F1$ string configurations those are stretched simultaneously along η and χ direction. Our purpose would be to check whether the above configuration (58) allows a sustainable configuration in the large $P(\gg 1)$ limit.

The corresponding Lagrangian density turns out to be

$$\mathcal{L}_P=f_1-f_2\sin^2\chi+f_2\chi'^2+f_3\eta'^2-2f_4\sin\chi\chi'. \tag{59}$$

Below, we note down the χ equation of motion that readily follows from (59)

$$f_2\chi''=-\frac{f_4}{2}\sin 2\chi-\partial_\eta f_2\eta'\chi'+\partial_\eta f_4\sin\chi\eta'. \tag{60}$$

The corresponding Virasoro constraint reads as

$$-f_1+f_2\chi'^2+f_2\sin^2\chi+f_3\eta'^2\approx 0. \tag{61}$$

Below we investigate each of the above equations (60)–(61) considering both the examples of single kink as well as quivers with a plateau.

1. $\tilde{T}_{N_c,P}$ quivers

Let us explore (60) in the holographic limit $P\gg 1$. An expansion of $f_4(\sigma,\eta)$ in the holographic limit reveals

$$f_4(\sigma\sim 0,\eta)|_{P\gg 1}\sim\frac{\pi^3\eta^3}{2P^2\log 2}+\mathcal{O}(1/P^4), \tag{62}$$

which together with (51) yields an equation of the form

$$\frac{\chi''}{\chi'}+\frac{2\eta'}{\eta}\approx 0, \tag{63}$$

that has a simple solution of the form

$$\chi'(\tilde{\sigma})\sim\frac{\mathcal{C}}{\eta^2}+\mathcal{O}(1/P), \tag{64}$$

where $\mathcal{C}$ is a constant of integration.

Notice that, the function (64) is singular as η approaches zero. Therefore, in order for the Lagrangian (59) to be well defined throughout the range $0\leq\eta\leq P$ one must set $\mathcal{C}=0$. In other words, $\chi(\tilde{\sigma})\sim$ constant in the strict holographic limit which naturally decouples the $F1$ string from the background NS-NS fluxes. Therefore, our findings essentially boil down to those in the absence of NS-NS fluxes.

To see this explicitly, we plug (64) into (61) which reveals

$$\eta'(\tilde{\sigma})\sim\frac{2\sqrt{3}\sqrt{\log 2}}{\pi}P+\cdots. \tag{65}$$

Using (65), the spectrum of long operators finally meet our expectation namely

$$\hat{\Delta}_{sk}\sim\frac{3}{2}P. \tag{66}$$

A similar calculation for the R-charge can be carried out in parallel which yields same answer as in (52).

2. $+_{P,N_c}$ quivers

We adopt similar methodology for quivers with a plateau where we estimate the metric functions $[f_i(\sigma\sim 0,\eta)]$ for the range $1\lesssim\eta\leq P$ as this produces dominant contributions to the integrals in the holographic limit.

Below, we summarize the metric functions $f_i(\sigma\sim 0,\eta)$ in the large $P(\gg\pi)$ limit

$$f_1(\sigma\sim 0,\eta)\sim 3\sqrt{\frac{3}{2}}\pi\sqrt{-\frac{\eta\log(\frac{\pi}{P})}{\log(\frac{\eta+1}{\eta-1})}}, \tag{67}$$

$$f_2(\sigma\sim 0,\eta)\sim\frac{-9\pi^2\eta^2\log(\frac{\pi}{P})}{2f_1(-2\log(\eta^2-1)+\eta\log(\frac{\eta+1}{\eta-1})-2\log(\frac{\pi}{P})+4+\log 16)}, \tag{68}$$

$$f_3(\sigma\sim 0,\eta)\sim\frac{9\pi^2}{4f_1}, \tag{69}$$

$$f_4(\sigma\sim 0,\eta)\sim\frac{\pi((5\eta^2+1)\log(\frac{\eta+1}{\eta-1})-2\eta)}{4(-2\log(\eta^2-1)+\eta\log(\frac{\eta+1}{\eta-1})-2\log(\frac{\pi}{P})+4+\log 16)}. \tag{70}$$

Using (67)–(70), it is now straightforward to show that in the strict holographic limit ($\frac{\pi}{P} \sim 0$) one has $f_4 \sim \partial_\eta f_4 \sim 0$. On the other hand, a straightforward computation reveals

$$\left.\frac{\partial_\eta f_2}{f_2}\right|_{P\to\infty} \sim \frac{1}{\eta} \tag{71}$$

which by virtue of (60) and following our previous discussion yields a solution of the form

$$\chi'(\tilde{\sigma}) \sim \mathcal{O}(1/P) \sim 0. \tag{72}$$

Therefore, to summarize, we conclude that in the strict holographic limit, the NS-NS flux does not affect the spectrum of long operators in $\mathcal{N} = 1$ SCFTs.

III. LIOUVILLIAN NONINTEGRABILITY

A. The algorithm

The strong coupling behaviour of both $\tilde{T}_{N_c,P}$ as well as $+_{P,N_c}$ quivers are encoded in the dynamics associated with type IIB strings those are described by the classical sigma model Lagrangian of the form (13). Therefore, one way to prove or disprove the integrability for these long quivers is to adopt some algorithm that classifies the underlying integrable structure associated with the phase space dynamics of these (semi)classical strings. Below, we elaborate more on this algorithm that drives the rest of our analysis.

To prove the integrability of the $2D$ sigma model (13) one needs to find the corresponding Lax pairs that reproduce the dynamics of the string in a consistent manner. This is indeed a nontrivial task. Therefore, instead of finding the Lax pairs, one should look for an alternative that disproves integrability for some particular embedding of these (semi)classical strings. This algorithm is named after Kovacic [18–19] that tells us some set of rules to classify the phase space dynamics and the associated integrable structure.

To apply the machinery due to Kovacic, the first step is to consider a consistent $1D$ truncation of the original sigma model (13) and study the resulting dynamics. The truncation usually results in a set of coupled partial differential equations which can be solved either numerically or analytically. Following the algorithm closely, one can in fact reduce these partial differential equations into a linear second order differential equation called the normal variational equation[8] (NVE)

$$\ddot{y}(\tau) + \mathcal{B}(\tau)\dot{y}(\tau) + \mathcal{A}(\tau)y(\tau) = 0, \tag{73}$$

where $\mathcal{A}$ and $\mathcal{B}$ are (complex) rational functions.

Given the NVE (73), one concludes that the classical phase of the string soliton is Liouvillian integrable if the corresponding solution can be expressed in terms of simple algebraic polynomials, harmonic functions, exponential or logarithmic functions—collectively known as Liouvillian form of solutions [20–26].

In his pioneering work [18], Kovacic has clearly stated about the necessary (but not sufficient) conditions for NVE to admit the Liouvillian form of solutions and prescribed an algorithm to construct such solutions based on the notion of the general $SL(2, C)$ group of invariance of (73). Let us elaborate on these conditions and summarize all the key features.

To understand these conditions properly, one needs to convert the NVE (73) into the familiar Schrödinger form

$$\dot{\omega}(\tau) + \omega^2(\tau) = V(\tau) = \frac{2\dot{\mathcal{B}} + \mathcal{B}^2 - 4\mathcal{A}}{4} \tag{74}$$

by redefining the original variable as

$$y(\tau) = e^{\int(\omega(\tau) - \frac{\mathcal{B}(\tau)}{2})d\tau}. \tag{75}$$

The NVE (73) allows a Liouvillian form of solution if the function $\omega(\tau)$ turns out to be a simple algebraic polynomial of degree 1, 2, 4, 6, or 12 [19]. In his original work [18], Kovacic clearly mentioned about those necessary conditions [26] that the potential function $[V(\tau)]$ must satisfy for the algorithm to be applicable in the first place.

These conditions essentially talk about the pole structure of $V(\tau)$ both for finite as well as large values of τ. They are summarized quite nicely in the Appendix of [26]. Once one of these criteria are satisfied then the algorithm can be applied to categorize the solutions of (74) into one of the above polynomials. On the other hand, if none of these (minimal) criteria are satisfied, then the analytic solution of (73) turns out to be non-Liouvillian and hence the corresponding phase space dynamics is nonintegrable.

Below, we elaborate on this taking specific examples of $\mathcal{N} = 1$ linear quivers in $5D$.

B. 1D reduction

We begin by considering a consistent $1D$ reduction of the original sigma model (13). To this end, we propose an embedding of the following form

$$t = \tau; \quad \eta = \eta(\tau); \quad \chi = \chi(\tau); \quad \xi = \ell\tilde{\sigma}, \tag{76}$$

where, we place the string soliton at the center of AdS_6 and restrict ourselves to the $\sigma = 0$ plane of the internal manifold $\mathcal{M}_4$. For simplicity, we consider the coupling of the string with the metric and the background NS-NS flux.

Using (76), the Lagrangian density for the reduced model turns out to be

[8]Here, by "dot" we mean derivative with respect to τ.

$$\mathcal{L}_P^{(1d)} = f_1\dot{t}^2 - f_2\dot{\chi}^2 - f_3\dot{\eta}^2 + \ell^2 f_2 \sin^2\chi + 2\ell f_4 \sin\chi\dot{\chi}. \quad (77)$$

Below, we note down the conjugate momenta

$$p_t = E = 2\dot{t} f_1, \quad (78)$$

$$p_\chi = -2f_2\dot{\chi} + 2\ell f_4 \sin\chi, \quad (79)$$

$$p_\eta = -2f_3\dot{\eta}, \quad (80)$$

that lead to the Hamiltonian density of the following form

$$-\mathcal{H}^{(1d)} = -\frac{E^2}{4f_1} + \frac{p_\eta^2}{4f_3} + \frac{1}{4f_2}(p_\chi - 2\ell f_4 \sin\chi)^2 + \ell^2 f_2 \sin^2\chi. \quad (81)$$

Below, we note down the equations of motion that readily follow form (77)

$$2f_3\ddot{\eta} = \partial_\eta f_2(\dot{\chi}^2 - \ell^2\sin^2\chi) - \partial_\eta f_3\dot{\eta}^2 - 2\ell\partial_\eta f_4 \sin\chi\dot{\chi} - \partial_\eta f_1, \quad (82)$$

$$-f_2\ddot{\chi} = \partial_\eta f_2\dot{\eta}\dot{\chi} + \ell^2 f_2 \sin\chi\cos\chi - \ell\partial_\eta f_4\dot{\eta}\sin\chi. \quad (83)$$

Finally, we note down the Virasoro constraints associated with the sigma model

$$-\mathcal{H}^{(1d)} = T_{\tau\tau} = -f_1 + f_3\dot{\eta}^2 + f_2\dot{\chi}^2 + \ell^2 f_2\sin^2\chi = 0, \quad (84)$$

$$T_{\tau\tilde{\sigma}} = 0. \quad (85)$$

A straightforward computation further reveals

$$\partial_\tau T_{\tau\tau} = -2\partial_\eta f_1\dot{\eta} = 0, \quad (86)$$

which therefore demands that for (76) to be a consistent embedding one must set $\eta = \eta_s =$ constant. In other words, the consistency requirement of the Virasoro constraint (86) confines the stringy dynamics over the submanifold $R\times S^2$. This further restricts the phase space dynamics of the string soliton to the two-dimensional subspace (of the full four-dimensional phase space) characterized by $\{p_\eta = 0, \eta = \eta_s\}$.

As we shall see, the reduced sigma model (77) allows two possible forms of NVEs. The solitonic configuration fails to be Liouvillian integrable if one of these NVEs does not meet the Kovacic's criteria those were elaborated above.

C. NVEs

1. Case I

In order to arrive at the corresponding NVEs, we choose to work with the invariant plane $\{p_\chi = 0, \chi = 0\}$ [20–26] in the phase space and consider fluctuations $[y(\tau)]$ normal to this plane. These fluctuations result in what we identify as NVEs those were mentioned previously in (73). Notice that the above subspace naturally solves (83) as $\chi = \dot{\chi} = \ddot{\chi} = 0$.

It is indeed quite straightforward to figure out this constant (η_s) for the given choice of phase space variables. A straightforward substitution into (82) reveals the condition

$$\partial_\eta f_1(\sigma\sim 0, \eta = \eta_s) \sim 0. \quad (87)$$

For $\tilde{T}_{N_c,P}$ quivers (21), the condition (87) reveals

$$\partial_\eta f_1(\sigma\sim 0, \eta=\eta_s)|_{P\gg 1} \sim -\frac{\pi^2\eta_s\sqrt{\frac{3}{\log 2}}}{8P} - \frac{\pi^4(\eta_s^2+1)\eta_s}{128P^3(\sqrt{3}\log^{\frac{3}{2}}2)} + \cdots, \quad (88)$$

which allows a trivial real solution as, $\eta_s \sim 0$.

For the range, $\eta \geq 1$, a similar analysis for $+_{P,N_c}$ quivers (32) reveals an equation

$$(\eta_s^2 - 1)\log\left(\frac{\eta_s+1}{\eta_s-1}\right) + 2\eta_s = 0, \quad (89)$$

which can be solved using the method of transcendental equations.

Finally, considering fluctuations $\delta\chi \sim y(\tau)$ about this invariant plane $\{p_\chi = 0, \chi = 0\}$, and retaining ourselves only up to leading-order one finds simple harmonic motion (with a unique frequency $\varpi \sim \ell$) of the following form

$$\ddot{y}(\tau) + \varpi^2 y(\tau) \approx 0, \quad (90)$$

which guarantees the trivial integrability of the type IIB string soliton under consideration.

In fact, this result is quite reminiscent of what has been observed previously in the context of type IIB $AdS_5\times S^5$ superstrings [20]. One therefore do not in fact need to go through all the details of Kovacic's algorithm those were mentioned previously as the power of differential Galois theory confirms the underlying integrable structure of (90).

2. Case II

We now look for a different possibility, where we try to figure out the NVEs considering an expansion about some fixed $\{p_\eta, \eta\}$ plane of the four dimensional phase space.

To start with, an obvious choice would be look for solutions subjected to the constraint $p_\eta \sim \dot{\eta} = 0$. A natural choice that is consistent with this constraint also amounts to set $\ddot{\eta} = 0$. Finally, a straightforward computation reveals that, $\partial_\eta f_i|_{\eta=0} = 0$ for $i = 1, 2, 3, 4$.

To summarize, we therefore conclude that $\eta = \dot{\eta} = \ddot{\eta} = 0$ is a consistent choice to start with which also solves the η-equation (82). Our goal would be to consider fluctuations about this $\{p_\eta = 0, \eta = 0\}$ plane and obtain the corresponding NVE.

Substituting this ansatz into (83), we obtain the corresponding solution to the χ- equation in terms of Jacobi amplitudes

$$\chi(\tau) = \mathrm{am}\left(\sqrt{(c_1 + \ell^2)(c_2 + \tau)^2}\,\middle|\,\frac{\ell^2}{c_1 + \ell^2}\right), \quad (91)$$

where c_1 and c_2 are the integration constants.

Using (91), we finally arrive at the NVE corresponding to $\tilde{T}_{N_c,P}$ quivers (21)

$$\ddot{y}(\tau) + \mathcal{A}(\tau) y(\tau) \approx 0, \quad (92)$$

where we identify the coefficient as

$$\mathcal{A}(\tau) = 2\ell^2 \sin^2\chi - c_1 - \frac{1}{4}. \quad (93)$$

The general solution of (92) is quite complicated due to the presence of the function $\mathcal{A}(\tau)$, hence the corresponding solution is non-Liouvillian. This particular string embedding therefore clearly indicates the signature of nonintegrability in the system.

Setting the integration constants to zero, and considering an expansion for small parameter range ($\tau \ll 1$) it is possible to simplify the function

$$\begin{aligned}\mathcal{A}(\tau) &\sim 2\ell^2 \tanh^2\left(\sqrt{\ell^2\tau^2}\right) - \frac{1}{4}\\ &\sim 2\ell^4\tau^2 - \frac{1}{4},\end{aligned} \quad (94)$$

which leads to solutions in terms of special parabolic cylindrical functions of the form

$$\begin{aligned} y(\tau) = {}& c_1 D_{-\frac{1}{2}+\frac{i}{8\sqrt{2}\ell^2}}\left((1+i)\sqrt{4}2\ell\tau\right)\\ &+ c_2 D_{-\frac{1}{2}-\frac{i}{8\sqrt{2}\ell^2}}((-2)^{3/4}\ell\tau). \end{aligned} \quad (95)$$

Looking back at the Schrödinger form (74), we notice that the potential function $V(\tau) = -\mathcal{A}(\tau)$ which makes the exact solution of $\omega(\tau)$ quite difficult. In fact, for the small parameter range $\tau \ll 1$, the solution manifests itself in the form of special parabolic cylindrical functions those were mentioned in (95). This further confirms the non-Liouvillian nature of solutions for the NVE (92).

To summarize, our analysis reveals the existence of at least one particular phase space configuration that does not meet the Liouvillian integrability criteria those were mentioned previously. Based on the notion of holography, this naturally leads us to conjecture about the nonintegrability of $\mathcal{N} = 1$ linear quivers in $5D$.

IV. NUMERICS

We now aim to decode the signatures of the above nonintegrability in terms of various physical phenomena associated with the dynamical phase space under consideration. One natural quest along this direction would be to search for possibilities of a chaotic motion for these type IIB strings by computing appropriate chaos indicators.

For the purpose of our present analysis, we look for two such indicators namely (i) the Lyapunov exponent and (ii) the Poincaré section. Below, we elaborate on each of these entities in detail. Finally, it is noteworthy to mention that the nonintegrability does not necessarily imply a chaotic motion, although the reverse is always true.

A. Chaos

The purpose of this section is to complement our analytical finding through numerics. In particular, we estimate the Lyapunov exponents (λ) for the type IIB strings under consideration. This amounts of solving the set of equations (82)–(83) for a given choice of the initial conditions. These initial conditions are set in such a manner so that the Hamiltonian constraint (81) vanishes identically. This naturally identifies the corresponding energy (E) of the string soliton and/or the long quiver. For technical simplicity, we explore these exponents for $\tilde{T}_{N_c,P}$ quivers (21) only.

The nonzero Lyapunov exponent, in some sense, is a measure of the chaotic dynamics associated with a Hamiltonian system [28–31]

$$\lambda = \lim_{\tau\to\infty} \lim_{\Delta X_0 \to 0} \frac{1}{\tau} \log \frac{\Delta X(X_0, \tau)}{\Delta X(X_0, 0)}. \quad (96)$$

Typically, (96) serves the purpose of a quantitative measurement of the rate of separation between two nearby trajectories (in the phase space) for a small change in the initial conditions. Here, X_0 corresponds to the initial phase space data while the function $\Delta X(X_0, \tau)$ measures the separation between two infinitesimally close trajectories at sufficiently late times, for a small change in the initial conditions.

Notice that, since the phase space of the present solitonic configuration is four dimensional $\{\eta, \chi, p_\eta, p_\chi\}$ therefore in principle there exist four Lyapunov exponents for the system whose sum vanishes to zero namely $\sum_{i=1}^4 \lambda_i = 0$.

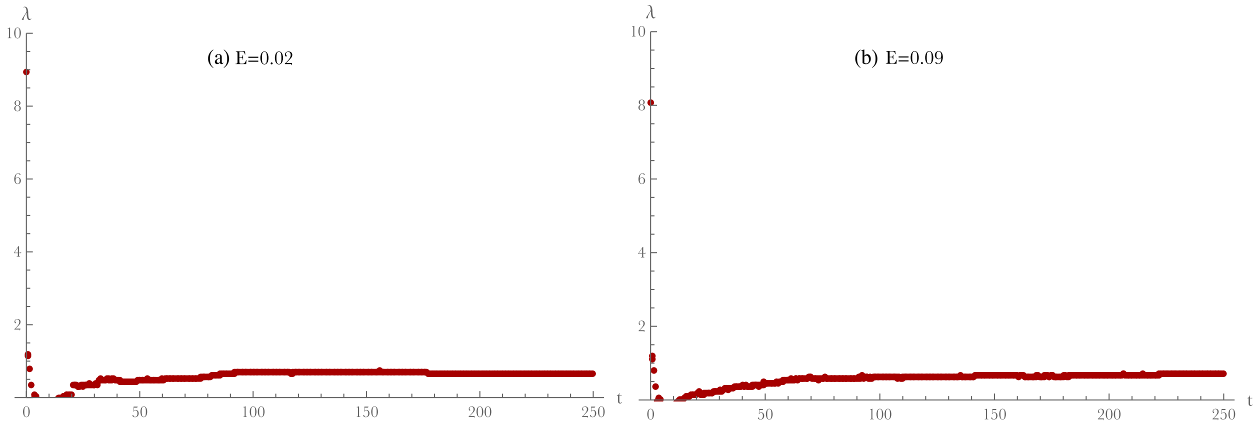

FIG. 1. We plot the Lyapunov exponents (λ) for $\tilde{T}_{N_c,P}$ quivers. We set $P=100$ and $\ell=5$ for each of these plots. (a) Single-kink profile that corresponds to a low-energy quiver, (b) Single-kink profile that corresponds to a higher excited state of the quiver. In the dual string theory picture, these plots correspond to strings those are less energetic and are located far away from the flavor D7-branes.

However, for the present analysis, we look for the largest possible Lyapunov associated with the solitonic configuration which is sufficient to convince about the chaotic dynamics of the phase space.

To begin with, we place the string soliton near the north pole of S^2 (as this naturally reduces the energy of the string) and explore the time evolution of the system. The initial conditions for Fig. 1(a) correspond to setting, $\chi(0)=0.05, \eta(0)=0.01, \dot{\chi}(0)=0.01$ and $\dot{\eta}(0)=0.001$. These initial conditions suggest that we place the string solitons far away from the flavor D7 branes. This fixes the energy of the string soliton to be $E\sim 0.02$ such that the constraint (84) is identically satisfied. From Fig. 1(a), it is quite evident that the Lypunov (λ) asymptotically approaches to some nonzero value. This clearly signifies the onset of chaos and hence nonintegrability associated with the solitonic configuration.

We further excite these strings (Fig. 1(b)) by placing them slightly away from the north pole. The initial conditions in this case correspond to setting $\chi(0)=0.2, \eta(0)=0.01, \dot{\chi}(0)=0.01$ and $\dot{\eta}(0)=0.001$. This fixes the energy of the string $E\sim 0.09$ which suggests that these solitons posses larger energy than those previous ones. Like before, we observe a nonzero value of the Lyapunov exponent (λ) which signals the persistence of chaotic motion associated with these type IIB strings.

Let us now consider a situation in which strings are initially placed closer to the flavor D7-branes. This is achieved by choosing an appropriate initial condition for the holographic coordinate η. In Fig 2 we show the corresponding plots for the Lyapunov exponents as the string approaches closer to the location of the flavor D7-branes which for the present example corresponds to, $\eta\sim 100$. From Fig. 2 it is evident that the string becomes

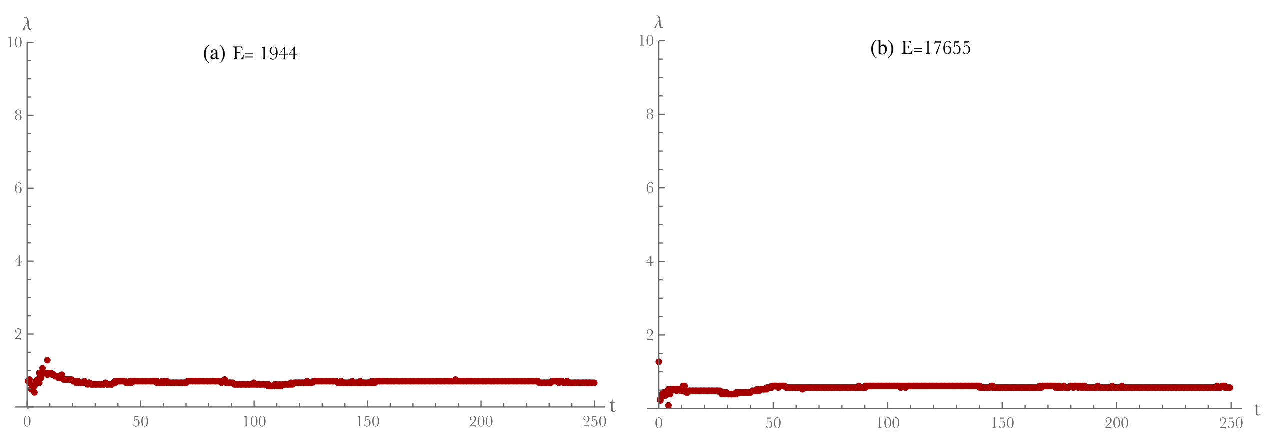

FIG. 2. We plot the Lyapunov exponents (λ) for $\tilde{T}_{N_c,P}$ quivers. We set $P=100$ and $\ell=5$ for each of these plots. (a) Single-kink profile that corresponds to a quiver with lower energy, (b) Single-kink profile that corresponds to a higher excited state of the quiver. In the dual string theory picture, these plots correspond to highly energetic strings those are located nearer to the flavor D7-branes.

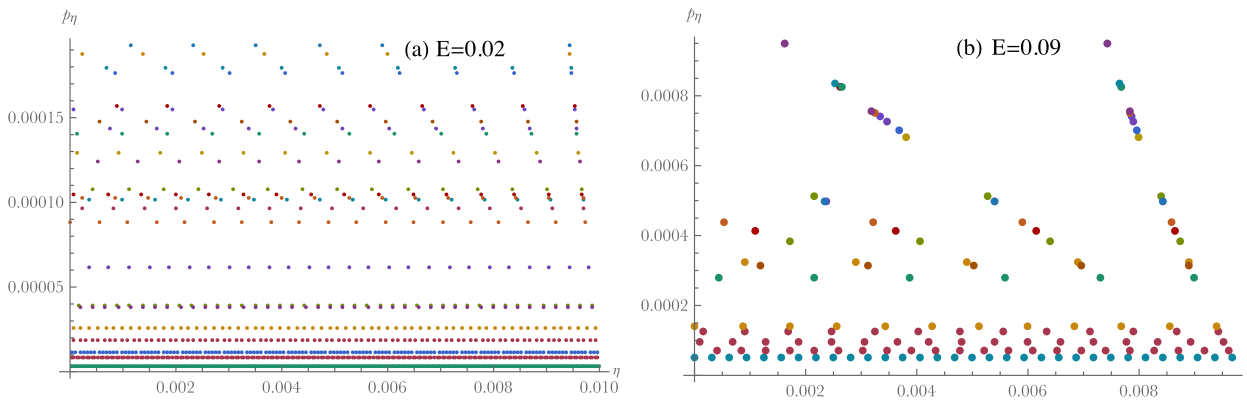

FIG. 3. We plot the Poincaré section for $\tilde{T}_{N_c,P}$ quivers. We set $P = 100$ and $\ell = 5$ for each of these plots. (a) Single-kink profile that corresponds to a low energy quiver, (b) Single-kink profile that corresponds to a higher excited state of the quiver. In the dual string theory picture, these plots correspond to a phase space configuration with less energetic strings those are located far away from the flavor D7-branes.

more and more energetic as it approaches the flavor branes. In other words, more energy needs to be supplied while moving the string closer to the location of the flavor branes. For our case, the initial positions for the string are set as $\eta(0) = 15$ [Fig. 2(a)] and $\eta(0) = 75$ [Fig. 2(b)] which correspond $E \sim 1944$ and $E \sim 17655$ respectively.

B. Poincaré section

Usually, for an integrable system the phase space trajectories lie on the KAM torus [28]. Generally, for an integrable system with N conserved charges ($\mathcal{Q}_i$)—the corresponding KAM torus is N dimensional. The trajectories over the KAM torus are completely specified in terms of these N conserved charges ($\mathcal{Q}_i$).

One elegant way to check the underlying integrable structure of the dynamical phase space is to take a $2D$ circular cross section of these KAM tori and see whether a large number of foliated circular KAM curves survive the external perturbation applied to the Hamiltonian of the system. These $2D$ cross sections of the foliated KAM tori are known as the Poincaré section. As per the KAM theorem, any nonintegrable perturbation added to the original integrable Hamiltonian destroys some of these KAM tori and thereby the foliated circular KAM curves those span the associated $2D$ Poincaré sections. As the strength of the nonintegrable deformation increases further, more and more KAM tori will be destroyed which will result in a seemingly random motion in the phase space.

In order to probe these Poincaré sections corresponding to $\mathcal{N} = 1$ quivers in $5D$, we solve the corresponding Hamiltonian dynamics that results from (82). Like before, we set the energy ($E = E_0$) of the string at some particular value which satisfies the Hamiltonian constraint (84) for some given set of initial conditions namely, $\eta(0) = 0.01$ and $p_\chi(0) = 0$. Given these initial conditions, we generate a random data set by choosing $p_\eta \in [0, 10]$ which fixes the corresponding $\chi(0)$ such that the constraint (84) is always satisfied.[9]

Finally, with the help of this initial data set, we carry out a numerical simulation of the Hamilton's equations of motion

$$\dot{\chi} = -\frac{1}{2f_2}(p_\chi - 2\ell f_4 \sin\chi), \tag{97}$$

$$\dot{p}_\chi = \ell^2\left(f_2 + \frac{f_4^2}{f_2}\right)\sin 2\chi - \frac{\ell f_4}{f_2}p_\chi \cos\chi, \tag{98}$$

$$\dot{\eta} = -\frac{p_\eta}{2f_3}, \tag{99}$$

$$\begin{aligned}\dot{p}_\eta = &\frac{E^2}{4f_1^2}\partial_\eta f_1 - \frac{p_\eta^2}{4f_3^2}\partial_\eta f_3 - \frac{\partial_\eta f_2}{4f_2^2}(p_\chi - 2\ell f_4 \sin\chi)^2 \\ &- \frac{\ell}{f_2}\partial_\eta f_4 \sin\chi(p_\chi - 2\ell f_4 \sin\chi) \\ &+ \ell^2 \partial_\eta f_2 \sin^2\chi,\end{aligned} \tag{100}$$

and plot all the points on the $\{p_\eta, \eta\}$ plane every time the trajectories pass through $\chi(t) = 0$ hyperplane. Which therefore represents a two-dimensional projection of a three dimensional hyperplane in the phase space.

For an integrable phase space configuration, a naive expectation would be to see the patches of circular KAM curves through this $2D$ projection. For the present analysis, the phase under consideration is four dimensional namely it

[9]Following our previous discussion, we stick to a configuration where the energy (E) of the soliton is the lowest possible. This corresponds to strings located away from the flavor D7-branes. For our purpose, it is sufficient to explore the Poincaré section for these low energy strings since the increase in E would enhance the possibilities of a more random motion which will destroy the associated KAM tori in the phase space.

is characterized by the axes $\{\chi, p_\chi, \eta, p_\eta\}$. In case of an integrable phase space, one would therefore expect the trajectories to be aligned along the two dimensional torus. Poincaré section of this torus would therefore unveil circular patches indicating the presence of different resonant tori.

From above Fig. 3 however, we do not see any evidence for such closed patches. As mentioned above, these Poincaré sections are obtained for strings sitting at the north pole ($\chi = 0$). As our analysis reveals, at low enough energies the trajectories in the phase space are more organized than its high-energy counterparts. Most of the string orbits are localized near the north pole of S^2 while the strings can move along the holographic direction (η) [Fig. 3(a)]. However, as the energy increases, the string starts moving with higher momentum (p_η) which by virtue of (100) reveals that the solitonic orbits are no longer localized near the north pole of S^2. In other words, the string starts moving randomly along the two sphere which results in a chaotic distribution of points along the Poincaré section [Fig. 3(a)]. The distribution of the these points (along Poincaré section) become more and more sparse as the corresponding energy (E) of the soliton increases.

To summarize, both these analyses accumulate enough evidence for the underlying nonintegrable structure of the $\mathcal{N} = 1$ SCFTs in $5D$.

V. SUMMARY AND FINAL REMARKS

To conclude, the present analysis reveals the existence of yet another class of strongly coupled nonintegrable SCFTs among the plethora of examples those are floating in the AdS/CFT landscape. These are the $\mathcal{N} = 1$ SCFTs living in $5D$ whose dual stringy counter part is described by type IIB supergravity solutions in $\mathrm{AdS}_6 \times S^2 \times \Sigma_{(2)}$.

Our analysis reveals that these $5d$ theories are Liouvillian nonintegrable in the sense of [18–19]. We further complement our claim through numerics where we estimate the corresponding Lyapunov exponent as well as the Poincaré section for the dynamical phase space under consideration. As a future remark, it is worthwhile to mention that it will be really nice to consider an S dual of these type IIB solutions and check whether the Liouvillian nonintegrability of the transformed background is still preserved. In fact, as a first step, one should construct the corresponding S dual background and perform an analysis of various field theory observables for example—the Page charges as well as the central charges corresponding to different $\mathcal{N} = 1$ quivers.

It will be also interesting to explore whether it is possible to implement the algorithm for a more generic class of quivers in $5D$. These are the quivers with unbalanced nodes —for example, $X_{N_c,M}$ theories as discussed in [10] and the (Y_{N_c}) quivers which are not S dual to themselves. In principle, the algorithm should be also be applicable for these theories based on the notion of the $SL(2,C)$ invariance of the space of solutions for complex partial differential equations which emerge from studying the dynamics of the string soliton over complex manifold.

We hope to be able to address some of these issues in the near future.

ACKNOWLEDGMENTS

The author is indebted to the authorities of IIT Roorkee for their unconditional support towards researches in basic sciences. The author is thankful to Carlos Nunez and Christoph Uhlemann for their valuable as well as thoughtful comments on the draft. The author would like to acknowledge The Royal Society, UK for financial assistance. The author would also like to acknowledge the Grant No. SRG/2020/000088 received from The Science and Engineering Research Board (SERB), India.

APPENDIX A: NONINTEGRABILITY OF LONG EXTENDED STRINGS

Let us briefly discuss the Liouvillian nonintegrability for long strings passing through flavor D7-branes located along the internal manifold ($\mathcal{M}_4$) of the full type IIB solution. The dynamics of these strings are described in (17)–(18).

Clearly, a choice $\sigma'' = \sigma' = \sigma = 0$ solves (17) which we therefore choose to be the reference plane about which the normal fluctuations ($\delta\sigma \sim y(\tilde{\sigma})$) are considered.

Substituting this choice into (18), we find

$$\eta'' \approx \left(\ell^2 - \frac{1}{4}\right)\eta + \cdots, \tag{A1}$$

where we stick to the large P limit while taking the specific example of $\tilde{T}_{N_c,P}$ quivers (21).

The above equation (A1) is solved for

$$\eta_s(\tilde{\sigma}) \simeq e^{-\gamma\tilde{\sigma}} + \mathcal{O}(1/P^2), \tag{A2}$$

where, $\gamma = \sqrt{\ell^2 - \frac{1}{4}}$.

Using (A2), the corresponding NVE turns out to be

$$y''(\tilde{\sigma}) + \mathcal{B}(\tilde{\sigma})y'(\tilde{\sigma}) + \mathcal{A}(\tilde{\sigma})y(\tilde{\sigma}) \approx 0, \tag{A3}$$

where the individual coefficients are identified as

$$\mathcal{B}(\tilde{\sigma}) = \frac{\pi^2\eta_s\eta_s'}{24P^2\log 2}, \tag{A4}$$

$$\mathcal{A}(\tilde{\sigma}) = -\left(\frac{1}{2} + \frac{\pi^2(\ell^2\eta_s^2 + \eta_s'^2)}{24P^2\log 2}\right). \tag{A5}$$

Clearly, the general solution of (A4) is non-Liouvillian. However, if we retain ourselves to the strict supergravity

($P \to \infty$) limit then the solution is of course Liouvillian, $y(\tilde{\sigma}) \sim e^{\frac{\tilde{\sigma}}{\sqrt{2}}}$. This is the limit in which the dispersion relation(s) (30) has been computed.

As a special note, below we express the potential function associated with the corresponding Schrödinger form

$$-V(\tilde{\sigma}) \simeq -\frac{1}{2} + \frac{\pi^2 \ell^2}{24P^2 \log 2} e^{-2\gamma\tilde{\sigma}} + \mathcal{O}(1/P^4), \qquad \text{(A6)}$$

which reveals a solution of (74) in terms of special functions namely a combination of Bessel functions coupled together with the Gamma functions. On the other hand, in the strict holographic limit ($P \to \infty$), the solution $[\omega(\tilde{\sigma})]$ corresponding to the Schrödinger equation (74) manifests itself as a polynomial of degree one, which confirms the Liouvillian integrability of the (long) string soliton in the above limit.

To summarize, we notice that it is the presence of flavor D7-branes which spoils the integrability. Setting, $P \to \infty$ corresponds to the fact that we place the flavor branes at infinity—as a consequence of this the string never meets the flavor branes. This is the limit in which the dispersion relation(s) (30) has been obtained. These are the massive string states which in fact cannot be excited.

APPENDIX B: A NOTE ON THE LARGE σ LIMIT

Below, we enumerate the metric functions $[f_i(\sigma,\eta)]$ and their derivatives in the large σ limit. Given the potential function as in (23), the corresponding metric functions read as

$$f_1(\sigma,\eta) \sim \frac{3\sqrt{3}P}{2} + \frac{1}{4}\sqrt{3}3\pi\sigma + \mathcal{O}(1/P), \qquad \text{(B1)}$$

$$f_2(\sigma,\eta) \sim \frac{\sqrt{3}\pi^2\eta^2}{2P} + \mathcal{O}(1/P^2), \qquad \text{(B2)}$$

$$f_3(\sigma,\eta) \sim \frac{\sqrt{3}\pi^2}{2P} + \mathcal{O}(1/P^2), \qquad \text{(B3)}$$

$$f_4(\sigma,\eta) \sim \frac{4\pi^3\eta^3}{3P^2} + \mathcal{O}(1/P^3), \qquad \text{(B4)}$$

$$f_5(\sigma,\eta) \sim -\frac{3(\pi^3\eta^3 N_c)}{2P^2} + \mathcal{O}(1/P^3), \qquad \text{(B5)}$$

$$f_6(\sigma,\eta) \sim \frac{4N_c^2}{3} + \mathcal{O}(1/P), \qquad \text{(B6)}$$

$$f_7(\sigma,\eta) \sim -2N_c + \mathcal{O}(1/P). \qquad \text{(B7)}$$

Using the above metric forms (B1)–(B7), we find

$$\ddot{\eta} \approx \eta(\dot{\chi}^2 - \ell^2 \sin^2\chi), \qquad \text{(B8)}$$

$$-\eta\ddot{\chi} \approx 2\dot{\eta}\dot{\chi} + \ell^2\eta\sin\chi\cos\chi. \qquad \text{(B9)}$$

In order to check the Liouvillian nonintegrability criteria, we set $\ddot{\chi} = \dot{\chi} = \chi = 0$ which clearly solves (B9). In other words, we choose to work with an invariant plane $\{p_\chi = 0, \chi = 0\}$ in the phase space and thereafter consider fluctuations about this plane.

Given the above choice, from (B8) we find

$$\eta(\tau)|_{\chi \sim 0} \sim a\tau + b. \qquad \text{(B10)}$$

Substituting (B10) into (B9) and considering fluctuations $\delta\chi \sim y(\tau)$, the corresponding NVE turns out to be

$$\ddot{y}(\tau) + \mathcal{B}(\tau)\dot{y}(\tau) + \mathcal{A}(\tau)y(\tau) \approx 0, \qquad \text{(B11)}$$

where we define coefficients as $\mathcal{B}(\tau) = \frac{2a}{a\tau+b}$ and $\mathcal{A}(\tau) = \ell^2 < 0$.

The corresponding solution turns out to be Liouvillian namely

$$y(\tau) \sim \frac{e^{-\sqrt{-\ell^2}\tau}\left(\frac{c_2 e^{2\sqrt{-\ell^2}\tau}}{\sqrt{-\ell^2}} + 2c_1\right)}{2(a\tau+b)}; \quad |\tau| \ll 1. \qquad \text{(B12)}$$

The potential function for the Schrödinger equation (74) turns out to be

$$V(\tau) = -\ell^2, \qquad \text{(B13)}$$

which is quite analogous to the case of simple harmonic motion as discussed in Sec. III C 1 which for small enough fluctuations $|y(\tau)| \ll 1$ yields a solution of the form

$$\omega(\tau) \sim -\ell^2\tau \qquad \text{(B14)}$$

which is a polynomial of degree one.

Let us now look at the other possibility namely to set, $\ddot{\eta} = \dot{\eta} = \eta = 0$ which clearly solves (B8). Substituting this choice into (B9) we find

$$\ddot{\chi} + 2g(\tau)\dot{\chi} + \ell^2 \sin\chi\cos\chi \approx 0, \qquad \text{(B15)}$$

where we introduce $\lim_{\eta\to 0}\frac{\dot{\eta}(\tau)}{\eta(\tau)} = g(\tau)$.

Naturally, any possible solution of (B15) is quite nontrivial which when substituted back into the NVE corresponding to fluctuations $[\delta\eta \sim y(\tau)]$ about the hyperplane $\{p_\eta = 0, \eta = 0\}$ yields solutions which are non-Liouvillian in nature.

APPENDIX C: SPACETIME SOLUTIONS [$f_i(\sigma,\eta)$] FOR $\eta > 1$

Below we summarize metric components for the range $1 \leq \eta \leq P$. We first note down

$$f_1(\sigma \sim 0, \eta) \sim \frac{3\sqrt{3}}{2\sqrt{2}}\pi\sqrt{\frac{a_1(\eta)}{b_1(\eta)}}, \tag{C1}$$

where we denote the individual entities as

$$a_1(\eta) = -(\eta^2+1)\log\left(\frac{\eta+1}{\eta-1}\right) + \eta(-2\log(\eta^2-1) + 6 + \log 16) - 4\eta\log\left(\frac{\pi}{P}\right), \tag{C2}$$

$$b_1(\eta) = \log\left(\frac{\eta+1}{\eta-1}\right). \tag{C3}$$

Next, we note down the function f_2 which can be schematically expressed

$$f_2(\sigma \sim 0, \eta) \sim \frac{a_2(\eta)}{b_2(\eta)} \tag{C4}$$

in terms of other functions

$$\frac{a_2(\eta)}{\sqrt{3}\pi} = \left((\eta^2+1)\log\left(\frac{\eta+1}{\eta-1}\right) - 2\eta(-\log(\eta^2-1) + 3 + \log(4)) + 4\eta\log\left(\frac{\pi}{P}\right)\right)^2, \tag{C5}$$

$$b_2(\eta) = c_2(\eta)\sqrt{\frac{-2(\eta^2+1)\log(\frac{\eta+1}{\eta-1}) + 4\eta(-\log(\eta^2-1) + 3 + \log(4)) - 8\eta\log(\frac{\pi}{P})}{\log(\frac{\eta+1}{\eta-1})}}, \tag{C6}$$

$$c_2(\eta) = -2(\eta^2+3)\log^2\left(\frac{\eta+1}{\eta-1}\right) + (-2\log(\eta^2-1) + 4 + \log(16))^2 + 16\log^2\left(\frac{\pi}{P}\right). \tag{C7}$$

Finally, we note down the metric component

$$f_3(\sigma \sim 0, \eta) \sim -\frac{a_3(\eta)}{b_3(\eta)}, \tag{C8}$$

where we identify individual entities as

$$a_3(\eta) = \sqrt{\frac{3}{2}}\pi\log\left(\frac{\eta+1}{\eta-1}\right)\sqrt{\frac{-(\eta^2+1)\log(\frac{\eta+1}{\eta-1}) + \eta(-2\log(\eta^2-1) + 6 + \log(16)) - 4\eta\log(\frac{\pi}{P})}{\log(\frac{\eta+1}{\eta-1})}}, \tag{C9}$$

$$b_3(\eta) = (\eta^2+1)\log\left(\frac{\eta+1}{\eta-1}\right) - 2\eta(-\log(\eta^2-1) + 3 + \log(4)) + 4\eta\log\left(\frac{\pi}{P}\right). \tag{C10}$$

---

[1] N. Seiberg, Five-dimensional SUSY field theories, nontrivial fixed points and string dynamics, Phys. Lett. B **388**, 753 (1996).

[2] A. Brandhuber and Y. Oz, The D-4—D-8 brane system and five-dimensional fixed points, Phys. Lett. B **460**, 307 (1999).

[3] Y. Lozano, E. Ó Colgáin, D. Rodríguez-Gómez, and K. Sfetsos, Supersymmetric AdS_6 via T Duality, Phys. Rev. Lett. **110**, 231601 (2013).

[4] A. Passias, A note on supersymmetric AdS_6 solutions of massive type IIA supergravity, J. High Energy Phys. 01 (2013) 113.

[5] E. D'Hoker, M. Gutperle, A. Karch, and C. F. Uhlemann, Warped $AdS_6 \times S^2$ in type IIB supergravity I: Local solutions, J. High Energy Phys. 08 (2016) 046.

[6] E. D'Hoker, M. Gutperle, and C. F. Uhlemann, Warped $AdS_6 \times S^2$ in Type IIB supergravity II: Global solutions and five-brane webs, J. High Energy Phys. 05 (2017) 131.

[7] E. D'Hoker, M. Gutperle, and C. F. Uhlemann, Warped $AdS_6 \times S^2$ in Type IIB supergravity III: Global solutions with seven-branes, J. High Energy Phys. 11 (2017) 200.

[8] M. Fluder and C. F. Uhlemann, Evidence for a 5d F-theorem, J. High Energy Phys. 02 (2021) 192.

[9] M. Gutperle and C. F. Uhlemann, Surface defects in holographic 5d SCFTs, J. High Energy Phys. 04 (2021) 134.

[10] C. F. Uhlemann, Wilson loops in 5d long quiver gauge theories, J. High Energy Phys. 09 (2020) 145.

[11] C. F. Uhlemann, Exact results for 5d SCFTs of long quiver type, J. High Energy Phys. 11 (2019) 072.

[12] C. F. Uhlemann, AdS_6/CFT_5 with O7-planes, J. High Energy Phys. 04 (2020) 113.

[13] M. Gutperle, C. Marasinou, A. Trivella, and C. F. Uhlemann, Entanglement entropy vs. free energy in IIB supergravity duals for 5d SCFTs, J. High Energy Phys. 09 (2017) 125.

[14] O. Bergman, D. Rodríguez-Gómez, and C. F. Uhlemann, Testing AdS_6/CFT_5 in Type IIB with stringy operators, J. High Energy Phys. 08 (**2018**) 127.

[15] M. Gutperle and N. Klein, A Penrose limit for type IIB AdS_6 solutions, J. High Energy Phys. 07 (2021) 073.

[16] A. Legramandi and C. Nunez, Electrostatic description of five-dimensional SCFTs, arXiv:2104.11240.

[17] F. Apruzzi, J. C. Geipel, A. Legramandi, N. T. Macpherson, and M. Zagermann, $\text{Minkowski}_4 \times S^2$ solutions of IIB supergravity, Fortschr. Phys. **66**, 1800006 (2018).

[18] J. J. Kovacic, An algorithm for solving second order linear homogeneous differential equations, J. Symb. Comput. **2**, 3 (1986).

[19] B. D. Saunders, An implementation of Kovacics algorithm for solving second order linear homogeneous differential equations, in *Proceedings of the Fourth ACM symposium on Symbolic and algebraic computation (SYMSAC 81), Snowbird, Utah, U.S.A., 57 August 1981*, pp. 105108.

[20] P. Basu and L. A. Pando Zayas, Analytic non-integrability in string theory, Phys. Rev. D **84**, 046006 (2011).

[21] A. Stepanchuk and A. A. Tseytlin, On (non)integrability of classical strings in p-brane backgrounds, J. Phys. A **46**, 125401 (2013).

[22] D. Giataganas, L. A. Pando Zayas, and K. Zoubos, On marginal deformations and non-integrability, J. High Energy Phys. 01 (2014) 129.

[23] K. Filippas, C. Núñez, and J. Van Gorsel, Integrability and holographic aspects of six-dimensional $\mathcal{N} = (1,0)$ superconformal field theories, J. High Energy Phys. 06 (2019) 069.

[24] D. Roychowdhury, Analytic integrability for strings on η and λ deformed backgrounds, J. High Energy Phys. 10 (2017) 056.

[25] C. Núñez, J. M. Penín, D. Roychowdhury, and J. Van Gorsel, The non-Integrability of Strings in Massive Type IIA and their Holographic duals, J. High Energy Phys. 06 (2018) 078.

[26] C. Nunez, D. Roychowdhury, and D. C. Thompson, Integrability and non-integrability in $\mathcal{N} = 2$ SCFTs and their holographic backgrounds, J. High Energy Phys. 07 (2018) 044.

[27] K. S. Rigatos, Nonintegrability of $L^{a,b,c}$ quiver gauge theories, Phys. Rev. D **102**, 106022 (2020).

[28] L. A. Pando Zayas and C. A. Terrero-Escalante, Chaos in the gauge/gravity correspondence, J. High Energy Phys. 09 (2010) 094.

[29] P. Basu and L. A. Pando Zayas, Chaos rules out integrability of strings on $AdS_5 \times T^{1,1}$, Phys. Lett. B **700**, 243 (2011).

[30] P. Basu, D. Das, and A. Ghosh, Integrability lost, Phys. Lett. B **699**, 388 (2011).

[31] P. Basu, D. Das, A. Ghosh, and L. A. Pando Zayas, Chaos around holographic regge trajectories, J. High Energy Phys. 05 (2012) 077.